Analysis and Improvement of Direct-Conversion Transmitter Pulling Effects in Constant Envelope Modulation Systems

Chieh-Hsun Hsiao, *Student Member, IEEE*, Chien-Jung Li, *Member, IEEE*, Fu-Kang Wang, *Student Member, IEEE*, Tzyy-Sheng Horng, *Senior Member, IEEE*, and Kang-Chun Peng, *Member, IEEE*

***Abstract*—Elucidating how local oscillator (LO) pulling affects a wireless direct-conversion transmitter that uses constant envelope modulation is of concern for global system for mobile communication (GSM). Therefore, this paper presents a phase dynamic model for a phase-locked loop (PLL) under directly modulated self-injection to evaluate the degraded phase noise performance of an LO pulled by a feedback modulation signal from the power amplifier output. Additionally, based on theoretical analysis, the proposed model can instruct system designers on how to optimize PLL parameters, as well as introduce an inner self-injection to minimize the impact of pulling effects. The improved performance is verified by implementing a Gaussian minimum-shift keying transmitter for GSM applications. Furthermore, the theoretical and experimental results correlate well with each other.**

***Index Terms*—Direct-conversion transmitter (DCT), injection pulling, local oscillator (LO) pulling, phase-locked loop (PLL), phase noise, self-injection locking, signal quality.**

I. Introduction

A DIRECT-CONVERSION transmitter (DCT) is usually adopted in system-on-chip for wireless communication systems because of its high integration and low power consumption. Fig. 1 illustrates a simple RF transmitter architecture, which contains a local oscillator (LO), quadrature modulator, and power amplifier (PA). The LO is normally based on a phase-locked loop (PLL) frequency synthesizer to provide a pure sinusoidal carrier. The modulator modulates baseband in-phase (I) and quadrature (Q) data on the RF carrier, followed by the PA to boost the transmitted modulation signal power. However, because of the zero offset between the transmit signal and LO frequency, the LO has become susceptible to the PA output modulation interference, often causing the frequency pulling to corrupt the output spectrum and LO phase noise [1]–[4]. Despite various shielding and complex digital processing procedures [5]–[8] to increase the isolation between the LO and PA or to reduce the specific interfering signal as much as possible, no general solution is available thus far to eliminate the LO pulling effects in a DCT.

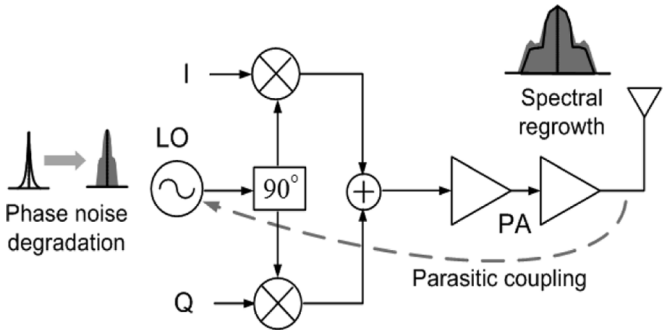

Fig. 1. Illustration of signal quality degradation owing to the LO pulling effects in a DCT.

Earlier, Adler [9] and others [10]–[20] studied the frequency pulling behavior of a free-running oscillator under injection of an independent sinusoidal signal. Many approaches have been developed recently to forecast the frequency pulling effects on various kinds of oscillators [16]–[20]. For instance, Razavi [14] considered a phase-locked oscillator (PLO) under an independent sinusoidal injection. Our previous work [20] provided theoretical and numerical approaches for accurately predicting the output spectra and phase noise variation of a PLO pulled by an independent modulation signal. Despite considerable effort to characterize the frequency pulling effects, however, a priority concern with respect to the LO pulling effects in a DCT is to develop an analytical system model for the LO pulled by an injected modulation signal with a carrier correlated with the LO output.

While investigating the DCT pulling phenomenon in constant envelope modulation systems, this work presents a phase dynamic model for a PLL under directly modulated self-injection. Based on the analytical approaches, we can directly analyze the pulling effects on deteriorating transmission signals and develop the relative solutions. The preliminary publication of this work [21] theoretically analyzed how to estimate the phase noise and error vector magnitude (EVM) degradation under the pulling effects. This paper considerably expands upon the result of [21]

Manuscript received July 03, 2010; revised October 05, 2010; accepted October 06, 2010. Date of publication November 09, 2010; date of current version December 10, 2010. This work was supported in part by the National Science Council, Taiwan, under Grant 97-2221-E-110-035-MY3, Grant 97-2628-E-110-041-MY3, Grant 98-2622-E-110-006-CC3, and Grant 99-2622-E-110-003-CC1, and by the Department of Industrial Technology, Taiwan, under Grant 98-EC-17-A-01-S1-104. This paper is an expanded paper from the IEEE MTT-S International Microwave Symposium, Anaheim, CA, May 23–28, 2010.

C.-H. Hsiao, C.-J. Li, F.-K. Wang, and T.-S. Horng are with the Department of Electrical Engineering, National Sun Yat-Sen University, Kaohsiung 80424, Taiwan (e-mail: d983010017@student.nsysu.edu.tw; jason@ee.nsysu.edu.tw).

K.-C. Peng is with the Department of Computer and Communication Engineering, National Kaohsiung First University of Science and Technology, Kaohsiung 811, Taiwan (e-mail: peterpkg@ccms.nkfust.edu.tw).

Color versions of one or more of the figures in this paper are available online at http://ieeexplore.ieee.org.

Digital Object Identifier 10.1109/TMTT.2010.2087351

by including a detailed method of directly modulated self-injection analysis. In particular, this paper develops a PLL parameter optimization method to minimize the pulling effects. Moreover, an inner self-injection approach is proposed for the first time to improve the pulling effects based on a dual self-injection PLL model.

The remainder of this paper is organized as follows. Section II describes how the pulling effects model is derived in the time and frequency domains. The proposed approach is analyzed in further detail for a DCT under injection pulling. Also, using the purposed model, the PLL parameters are characterized to achieve the optimal resistance to pulling effects. In Section III, we begin by introducing the inner self-injection approach. With the assistance of the frequency-domain dual self-injection PLL model, the operating principles of the proposed approach are also explicitly defined. Additionally, the theoretical calculation and experimental results regarding the phase noise and signal quality improvement are discussed. Section IV then demonstrates the improved results of the proposed approaches. Finally, Section V summarizes and concludes this paper.

II. Analysis Approach

This section introduces the phase dynamic model for a directly modulated self-injection PLL, which is the initial step to theoretically analyze the LO pulling effects in a DCT. A constant envelope modulation communication system is considered when the proposed model is used to characterize the deterioration of transmitted signal quality. The experimental results are provided for model validation.

III. LO Pulling Effects Model

Based on Adler's analysis [9] and previous approach [20], the voltage-controlled oscillator (VCO) output signal can be regarded as a vector rotating clockwise with an instantaneous beat frequency $d\alpha(t)/dt$ with respect to the injection frequency. The instantaneous VCO output frequency related to the instantaneous injection frequency can be expressed as

$$\omega_{\rm out}(t) = \frac{\omega_{\rm inj}(t) + d\alpha(t)}{dt} \tag{1}$$

where

$$\frac{d\alpha(t)}{dt} = -\frac{\omega_{\rm osc}(t)}{2Q}\frac{E_{\rm inj}}{E_{\rm osc}}\sin\alpha(t) + \Delta\omega_{\rm osc}(t) \tag{2}$$

is the well-known Adler's equation. In (2), $\omega_{\rm osc}(t)$ represents the inherent oscillation frequency determined by the tank circuit with a quality factor Q in a VCO. Additionally, $E_{\rm inj}$ and $E_{\rm osc}$ represent the injection signal $S_{\rm inj}$ and oscillation signal $S_{\rm osc}$ amplitude, respectively. Moreover, $\Delta\omega_{\rm osc}(t)$ denotes the undisturbed beat frequency. Fig. 2 illustrates the simplified model of an oscillator under injection and the relative signal vector representation.

In contrast with Adler's analysis, we proceed with the derivation by initially assuming that the inherent oscillation and injection frequency have an instantaneous variation $d\theta_0(t)/dt$ and $d\theta_i(t)/dt$, respectively. The undisturbed beat frequency in (2)

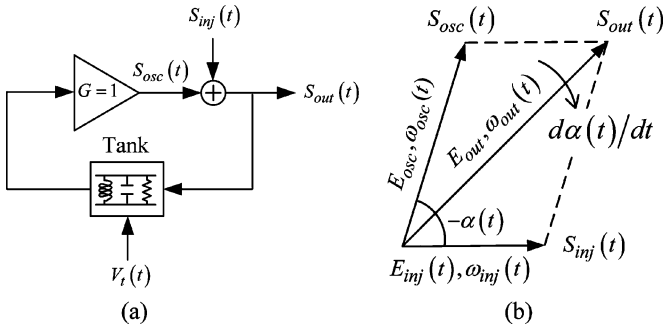

Fig. 2. (a) Block diagram of an oscillator under injection. (b) Vector diagram of the signals as specified in Adler's analysis.

can be rewritten as

$$\begin{aligned}\Delta\omega_{\rm osc}(t) &= \left[\frac{\omega_{\rm osc} + d\theta_0(t)}{dt}\right] - \left[\frac{\omega_{\rm inj} + d\theta_i(t)}{dt}\right] \\ &= \frac{\Delta\omega_{\rm osc} + d\theta_0(t)}{dt} - \frac{d\theta_i(t)}{dt}\end{aligned} \tag{3}$$

where $\Delta\omega_{\rm osc} = (\omega_{\rm osc} - \omega_{\rm inj})$ defines the frequency separation between inherent oscillation and injection center frequency. As mentioned earlier, the PLL is disrupted by the PA output modulation signal, which has a center frequency equal to the synthesized frequency, via a parasitic coupling path. Therefore, $\Delta\omega_{\rm osc}$ should be zero for applying in this work. Consider that $\omega_{\rm osc}(t)$ does not originate from a free-running oscillator, but rather from an LO controlled by a PLL. The PLL mechanism can dynamically correct the oscillation frequency via a tuning voltage $V_t(t)$, and thus, the instantaneous frequency variation $d\theta_0(t)/dt$ of the VCO can be replaced by $K_v V_t(t)$, where K_v is the tuning sensitivity of VCO. Assume that the VCO is finally phase locked with a weak injection. The assumptions can be mathematically restated as $K_v V_t(t) \ll \omega_{\rm osc}$ and $\sin\alpha(t) \ll 2QE_{\rm osc}/E_{\rm inj}$. Therefore, the subsequent LO output frequency $\omega_{\rm LO}(t)$ can be obtained and approximated as

$$\begin{aligned}\omega_{\rm LO}(t) &= [\omega_{\rm osc} + K_v V_t(t)] \cdot \left[1 - \frac{1}{2Q}\frac{E_{\rm inj}}{E_{\rm osc}}\sin\alpha(t)\right] \\ &\approx \omega_{\rm osc} + K_v V_t(t) - \omega_{LR}\beta(t)\end{aligned} \tag{4}$$

where

$$\omega_{LR} = \frac{\omega_{\rm osc}}{2Q}\frac{E_{\rm inj}}{E_{\rm osc}} \tag{5}$$

is interpreted as the locking range of a free-running oscillator [5]. In (4), $\beta(t)$ is equivalent to $\sin\alpha(t)$ and is regarded as an equivalent injection-induced source to cause frequency modulation in a PLL. Integrating (4) yields the resulting LO output phase as

$$\phi_{\rm LO}(t) = \omega_{\rm osc}t + K_v\int V_t(t)dt + \theta_0 - \omega_{LR}\int\beta(t)dt \tag{6}$$

where θ_0 represents an initial oscillation phase. Notably, the above equation interprets the resulting LO output phase as a combination of the phase-locking mechanism and the injection-locking process [20]. A different formulation for the coexistence of the phase and injection locking of oscillator can also

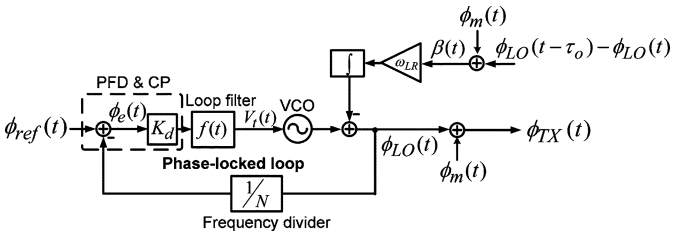

Fig. 3. Time-domain phase dynamics of a PLL under injection.

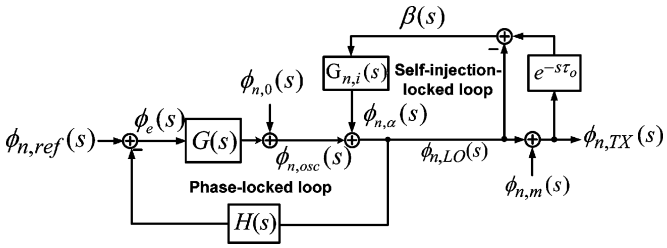

Fig. 4. Frequency-domain model for analyzing phase noise and modulation accuracy of a directly modulated self-injection PLL.

be found in [22], yielding a locking range expression different from (5) because of adding a feedback loop in the oscillator. In the following derivation, this work has an essential difference from [20] and [22] by considering a self-injection signal rather than an independent injection signal, as used in [20] and [22]. When the PLL enters the directly modulated self-injection locking state by inserting the LO output signal into the injection port of the VCO via a self-injection path, the instantaneous phase variation of the feedback interference signal S_{inj} can be considered as a delayed version of the instantaneous LO phase noise $\phi_{\text{LO}}(t)$ and DCT output phase modulation $\phi_m(t)$. With the assumptions of low LO phase noise and narrow modulation bandwidth, the equivalent injection-induced source $\beta(t)$ can be approximated as

$$\beta(t) = \sin\alpha(t) \approx \alpha(t) = \phi_{\text{LO}}(t-\tau_0) - \phi_{\text{LO}}(t) + \phi_m(t-\tau_0) \tag{7}$$

where τ_0 represents the time delay of the self-injection path.

Based on the above derivations, the phase dynamics with all signals of interest in the PLL under injection can be modeled as shown in Fig. 3, where K_d denotes the combined gain of the phase frequency detector (PFD) and the charge pump (CP), $f(t)$ represents the impulse response of the loop filter; N represents the divider modulus; $\phi_m(t)$ and $\phi_{\text{ref}}(t)$ express the phase modulation and phase of the reference, respectively; and $\phi_e(t)$ is the output phase error of the PFD. Although such a phase dynamic model does not include the PA gain and self-injection path loss, they both will influence the injection signal amplitude E_{inj}, and thus, the locking range ω_{LR}.

This work analyzes the DCT pulling effects in a constant envelop modulation system. Therefore, in this work, the power-amplified output signal is treated as a phase-modulated (PM) signal. The instantaneous phase modulation $\phi_m(t)$ of the PM signal can be extracted by using the vector signal analyzer (VSA). Therefore, we can develop a corresponding frequency-domain model for phase noise analysis of a directly modulated self-injection PLL by taking the Laplace transforms of (2), (6), and (7), as shown in Fig. 4.

In Fig. 4, $G(s) = K_d F(s) K_v/s$ and $H(s) = 1/N$ represent the PLL forward- and feedback-path transfer function, respectively; τ_0 denotes the self-injection path delay; and $G_{n,i}(s) = \omega_{LR}/s$ is an equivalent path gain for self-injection that is obtained from the Laplace transform of (6). $\phi_{n,\text{ref}}(s)$, $\phi_{n,0}(s)$, and $\phi_{n,\text{LO}}(s)$ denote the phase noise of the reference, oscillator, and LO output, respectively. Additionally, $\phi_{n,m}(s)$ and $\beta(s)$ refer to the Laplace-domain representation of $\phi_m(t)$ and $\beta(t)$, respectively, while $\phi_{n,\text{TX}}(s)$ represents the resulting phase response in the transmitter output. The dual-loop model shown in Fig. 4 is apparently a combination of the PLL and the self-injection-locked loop, while the LO phase noise $\phi_{n,\text{LO}}(s)$ can be formulated as

$$\phi_{n,\text{LO}}(s) = \phi_{n,\text{osc}}(s) + \phi_{n,\alpha}(s) \tag{8}$$

with

$$\begin{aligned}\phi_{n,\text{osc}}(s) &= \phi_e(s)G(s) + \phi_{n,o}(s) \\ &= [\phi_{n,\text{ref}}(s) - \phi_{n,\text{LO}}(s)H(s)]G(s) + \phi_{n,0}(s) \qquad (9)\\ \phi_{n,\alpha}(s) &= G_{n,i}(s)\beta(s) \\ &= G_{n,i}(s)[\phi_{n,\text{LO}}(s)(e^{-\tau_0 s}-1) + \phi_{n,m}(s)e^{-\tau_0 s}]. \qquad (10)\end{aligned}$$

Incorporating the preceding results into (8) leads to the overall LO phase noise as expressed in the following equations:

$$\begin{aligned}\phi_{n,\text{LO}}(s) = H_{n,\text{ref}}(s)\phi_{n,\text{ref}}(s) + H_{n,\text{osc}}(s)\phi_{n,0}(s) \\ + H_{n,\text{inj}}(s)\phi_{n,m}(s) \qquad (11)\end{aligned}$$

where

$$H_{n,\text{ref}}(s) = \frac{G(s)H_{n,o}(s)}{1+G(s)H(s)H_{n,o}(s)} \tag{12}$$

$$H_{n,\text{osc}}(s) = \frac{H_{n,o}(s)}{1+G(s)H(s)H_{n,o}(s)} \tag{13}$$

$$H_{n,\text{inj}}(s) = \frac{H_{n,i}(s)}{1+G(s)H(s)H_{n,o}(s)}. \tag{14}$$

Note that in (12)–(14), $H_{n,0}(s)$ and $H_{n,i}(s)$ are the self-injection-locked loop transfer functions and are given as

$$H_{n,0}(s) = \frac{1}{1+G_{n,i}(s)(1-e^{-s\tau_0})} \tag{15}$$

$$H_{n,i}(s) = \frac{G_{n,i}(s)e^{-s\tau_0}}{1+G_{n,i}(s)(1-e^{-s\tau_0})}. \tag{16}$$

where $G_{n,i}(s) = \omega_{LR}/s$ is the aforementioned equivalent path gain in the self-injection locked loop.

Equation (11) indicates that the LO phase noise is broken down into its three major noise components, i.e., the reference, oscillator, and PM injection. The noise transfer functions (12)–(14) are obviously in an interaction of the PLL transfer functions $G(s)$, $H(s)$, and the self-injection-locked loop

transfer functions $H_{n,0}(s)$ and $H_{n,i}(s)$. Overall, $H_{n,\mathrm{ref}}(s)$, $H_{n,\mathrm{osc}}(s)$, and $H_{n,\mathrm{inj}}(s)$ shows a property of low-pass, high-pass, and bandpass filtering with respect to $\phi_{n,\mathrm{ref}}(s)$, $\phi_{n,0}(s)$, and $\phi_{n,m}(s)$, respectively. With knowledge of the spectral power density for individual noise components, the overall LO phase noise power spectral density can be calculated by

$$S_{n,\mathrm{LO}}(\omega) = |H_{n,\mathrm{ref}}(j\omega)|^2 S_{n,\mathrm{ref}}(\omega) + |H_{n,\mathrm{osc}}(j\omega)|^2 \times S_{n,0}(\omega) + |H_{n,\mathrm{inj}}(j\omega)|^2 S_{n,m}(\omega) \quad (17)$$

where $S_{n,\mathrm{ref}}(\omega)$, $S_{n,0}(\omega)$, and $S_{n,m}(\omega)$ is the power spectral density of $\phi_{n,\mathrm{ref}}(s)$, $\phi_{n,0}(s)$, and $\phi_{n,m}(s)$, respectively. Degradation of the modulation accuracy in a transmitter can be estimated by evaluating the distortion of the transmitter output signal $S_{\mathrm{TX}}(\omega)$ spectrum. It can be found from Fig. 4 that $\phi_{\mathrm{TX}}(j\omega)$ is equivalent to $\phi_{n,m}(j\omega) + \phi_{n,\mathrm{LO}}(j\omega)$. Thus, obviously $S_{n,\mathrm{LO}}(\omega)$ is the cause of the distortion.

Notably, the frequency-domain model presented in [20] can also predict the similar filtering characteristics of the noise transfer functions. However, the model in [20] is based on an independent modulated injection. In contrast, the model shown in Fig. 4 considers a modulated self-injection to include the dependence of system noise on the self-injection path delay τ_0. With such a consideration, the proposed model in this work can predict the DCT pulling effects more accurately.

A. EVM Analysis

As discussed earlier, the power-amplified interference is simplified as a PM self-injection signal. Therefore, the interference's PM-to-PM influence dominates the deterioration of the transmitted signal quality. Based on the predicted phase noise power spectral density $S_{n,\mathrm{LO}}(\omega)$ using (17), degradation the EVM can be estimated by referring to [23] and [24]. By integrating $S_{n,\mathrm{LO}}(\omega)$ over a specific frequency span from f_{low} to f_{up}. The root mean square (rms) phase error can be found as

$$\sigma_v^2 = 2\int_{f_{\mathrm{low}}}^{f_{\mathrm{up}}} S_{n,\mathrm{LO}}(\omega)d\omega = 2\int_{f_{\mathrm{low}}}^{f_{\mathrm{up}}} v^2(\omega)d\omega \quad (18)$$

where $v(\omega)$ represents the voltage noise in relation to the carrier, which has a zero mean value. Additionally, σ_v denotes the standard deviation of the relative noise voltage. By definition, the rms phase error (σ_ϕ) and EVM can thus be calculated as

$$\sigma_\phi(\mathrm{deg}) = \frac{180}{\pi}\sigma_v = \frac{180}{\pi}\sqrt{2\int_{f_{\mathrm{low}}}^{f_{\mathrm{up}}} S_{n,\mathrm{LO}}(\omega)d\omega} \quad (19)$$

$$\mathrm{EVM} = \left(\frac{\pi}{180^\circ}\right)\cdot\sigma_\phi\cdot 100\%. \quad (20)$$

According to our analysis, the phase noise at the offset frequency close to the PM injection bandwidth more significantly impacts the EVM performance than at the other offset frequencies. Therefore, this observation inspires us to develop the following approaches.

B. PLL Parameters Impact

The experiment implements an S-band direct conversion transmitter to verify the correctness of our theoretical analysis.

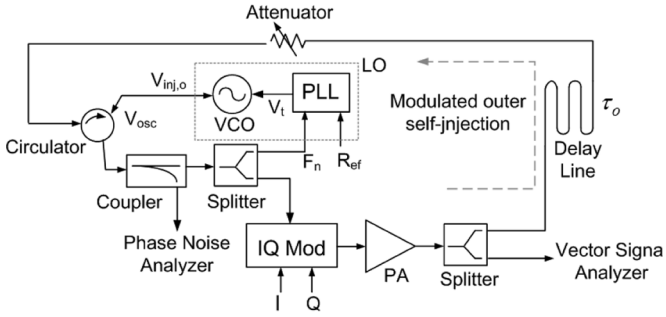

Fig. 5. Block diagram of the LO pulling test setup for a direct-conversion GMSK transmitter.

The proposed transmitter mainly includes an LO, IQ modulator, and PA. In the experiments, the LO is locked at 2.5 GHz, delivering an oscillation power of 0 dBm. This experiment is performed in Gaussian minimum-shift keying (GMSK) modulation with a 270.833-kb/s data rate, which is normally adopted in global system for mobile communication (GSM) systems. The baseband I and Q component signals are provided by an Agilent E4438C vector signal generator.

Fig. 5 illustrates the experimental setup for testing the transmitter pulling effects, indicating that the power-amplified output GMSK modulation signal is fed back to the VCO via a splitter, delay line, attenuator, and circulator to act as a modulated outer self-injection signal into the LO. The transmitter output is connected to the spectrum and VSA with the assistance of a coupler for simultaneously measuring the output spectrum and EVM. It is noted that the attenuator attenuation is controllable to adjust the injection power level. Additionally the self-injection signal is isolated from the LO output signal by using the circulator. By referring to (11) and (14), the influence of PM injection noise on LO phase noise is dependent on the PLL transfer functions. Therefore, an attempt is made to change the PLL parameters for reducing the impact of PM injection noise. In strategy, the magnitude of the PM injection noise transfer function $H_{n,\mathrm{inj}}(s)$ can be diminished as much as possible to ensure the optimal transmitted signal quality. The following introduces the measured and calculated results of an LO influenced by various interference conditions and PLL parameters.

Fig. 6(a) and (b) displays the magnitude response of noise transfer functions $H_{n,\mathrm{ref}}(j\omega)$, $H_{n,\mathrm{osc}}(j\omega)$, and $H_{n,\mathrm{inj}}(j\omega)$ by using (12)–(14) at a modulated outer self-injection power of -45 dBm and an outer self-injection path delay of 12.5 ns. In these figures, the dotted lines in blue (in online version), broken lines in red (in online version), and solid lines in black express the responses with PLL phase margin equal to 37°, 67°, and 85°, respectively. According to these figures, the magnitude of the dominant transfer function $H_{n,\mathrm{inj}}(s)$ near symbol rate frequency offset decreases with an increasing PLL phase margin. This finding implies that higher phase margin is more resistant to the pulling effects.

Fig. 6(c)–(e) summarizes the measurement and calculation results of the LO phase noise and EVM degradation under various PLL phase margins. Comparing these results reveals an excellent correlation. Consider the stability performance of the overall system, the phase margin is often chosen between

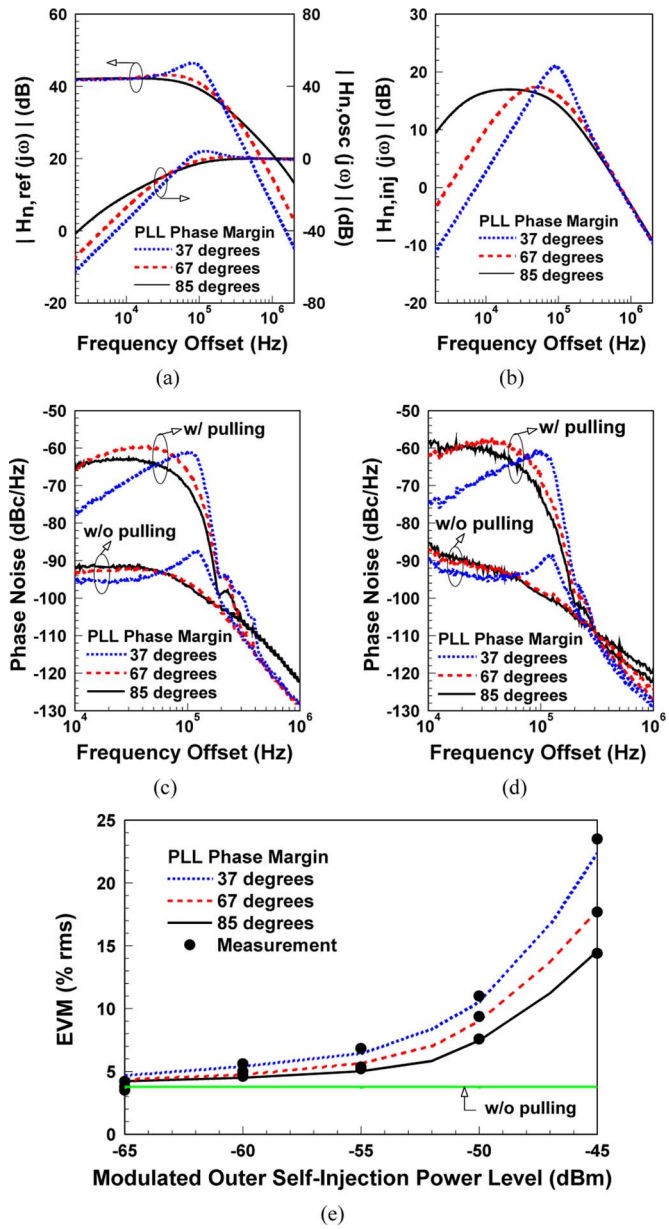

Fig. 6. Analysis of LO pulling effects and validation under various PLL phase margins. (a) Calculated magnitude of the reference and oscillator noise transfer functions. (b) Calculated magnitude of the PM injection noise transfer function. (c) Calculated LO phase noise. (d) Measured LO phase noise (e) Calculated and measured transmitter EVMs.

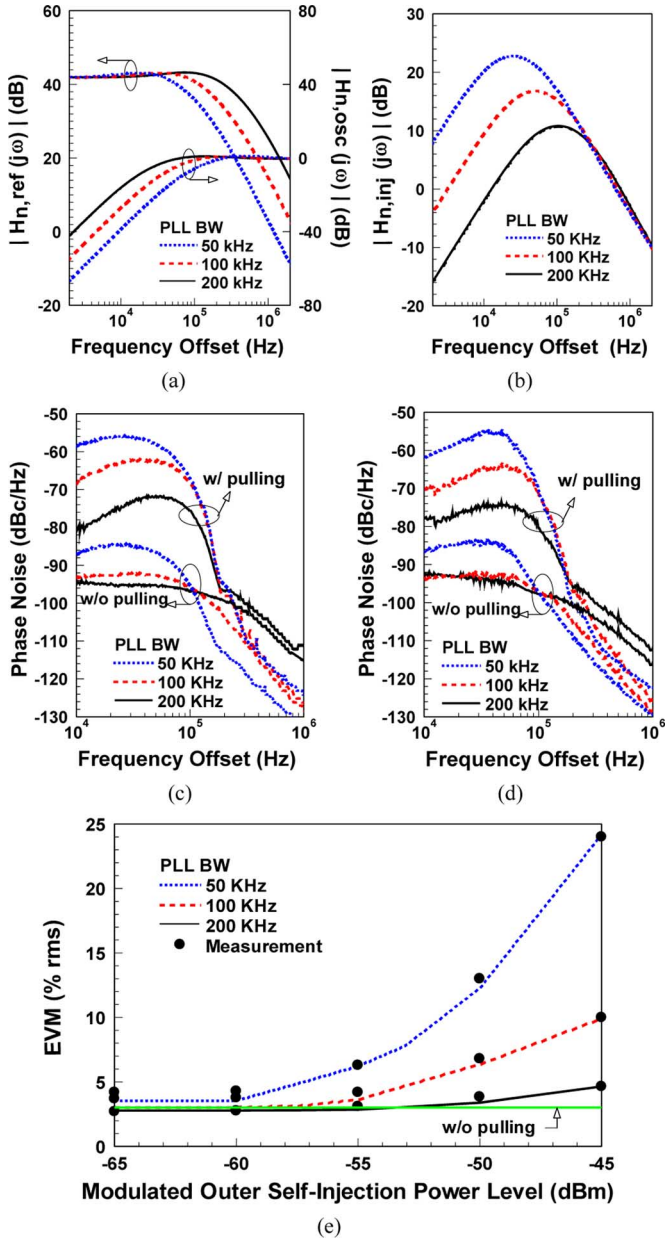

Fig. 7. Analysis of LO pulling effects and validation under various PLL bandwidths. (a) Calculated magnitude of the reference and oscillator noise transfer functions. (b) Calculated magnitude of the PM injection noise transfer function. (c) Calculated LO phase noise. (d) Measured LO phase noise (e) Calculated and measured transmitter EVMs.

30° and 50°, while a higher PLL phase margin leads to more reduction of the peak phase noise response at the expense of increasing the locking time. However, if the LO suffers from pulling effects to cause significant deterioration in transmitted signal quality, the typically chosen PLL phase margins have to be increased to achieve the best resistance to the pulling effects.

Fig. 7(a) and (b) shows the magnitude response of noise transfer functions $H_{n,\mathrm{ref}}(j\omega)$, $H_{n,\mathrm{osc}}(j\omega)$, and $H_{n,\mathrm{inj}}(j\omega)$ as the modulated outer self-injection power equals to -45 dBm and the outer self-injection path delay is 12.5 ns, while the dotted lines in blue (in online version), broken lines in red (in online version), and solid lines in black express the responses with PLL bandwidth equal to 50, 100, and 200 kHz, respectively. According to the above results, the magnitude of the dominant transfer function $H_{n,\mathrm{inj}}(s)$ decreases with an increasing PLL bandwidth at the frequency offset of concern, indicating that the impact of the PM injection noise becomes suppressed with a wider PLL bandwidth.

Fig. 7(c)–(e) shows the measurement and calculation results of the LO phase noise and EVM degradation under different PLL bandwidths. An excellent correlation can be obtained from these figures. Consider the stability performance of the overall system, the PLL bandwidth is typically chosen to be 5%–10% of the reference signal frequency. Additionally, designers often select the PLL bandwidth at the intersection offset frequency of the reference and VCO phase noise curves to ensure the optimum performance of phase noise. However, if the LO is significantly disturbed by the PA interference, the typically chosen

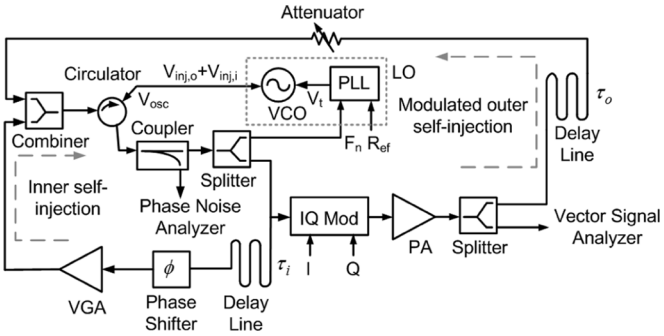

Fig. 8. Block diagram of the pulling test setup for the direct-conversion GMSK transmitter with an inner self-injection locked loop.

PLL bandwidths have to be increased to ensure the optimal pulling effects resistance.

IV. Improvement Approach

A few studies [25]–[28] have recently developed a self-injection approach to stabilize and reduce the phase noise for microwave oscillators. For instance, Chang [25] explained the phase-noise reduction as an intuitive result of the oscillator synchronization to serve as a re-inject stabilized signal. In other words, the self-injection mechanism can provide a correction signal to readjust oscillating condition. Importantly, the oscillator phase fluctuation can be reduced as long as satisfying the stable constraints of self-injection-locking. Of particular interest here is the dependency of the oscillator phase noise reduction extent upon different self-injection conditions. This characteristic will be exploited in the proposed approach to achieve substantial reduction in pulling effects, including LO phase noise degradation, spectral regrowth, and EVM degradation.

A. Inner Self-Injection Locked Loop

Fig. 8 depicts the experimental setup, which is used to demonstrate the improvement in LO phase noise and transmitted signal quality performance by applying an inner self-injection locked loop. In this figure, the difference from Fig. 5 is only that part of LO signal disturbed by PA output modulation signal is feedback to the VCO as part of injection signal to establish the inner self-injection locked loop. In this loop, a delay line, phase shifter, and variable controllable amplifier (VGA) are used to adjust the delay time, injection angle, and injection power to ensure the maximum amount of the transmitted signal quality improvement.

The dual self-injection PLL model for the experimental setup in Fig. 8 is shown in Fig. 9, while the inner self-injection locked loop is the proposed improved mechanism as the outer one is preserved to imitate the pulling phenomenon. In this figure, $G'_{n,i}(s)$, τ_i, and ϕ represent the equivalent path gain, delay time, and injection angle, respectively, of the inner self-injection locked loop, while the other parameters are used to describe the PLL and the modulated outer self-injection locked loop. The overall phase noise $\phi_{n,\mathrm{LO}}(s)$ can be rewritten as a combination of the PLL and two self-injection locked loops

$$\phi_{n,\mathrm{LO}}(s) = H_{n,\mathrm{ref}}(s)\phi_{n,\mathrm{ref}}(s) + H_{n,\mathrm{osc}}(s)\phi_{n,0}(s) + H_{n,\mathrm{inj}}(s)\phi_{n,m}(s) \quad (21)$$

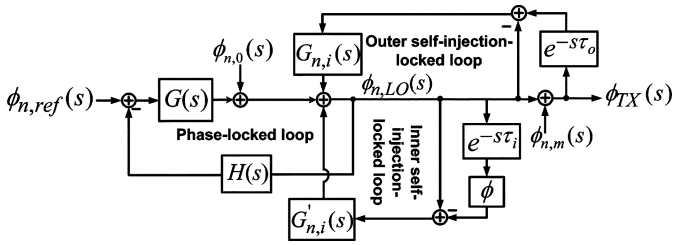

Fig. 9. Frequency-domain model for analyzing phase noise and modulation accuracy of a dual self-injection PLL.

where

$$H_{n,\mathrm{ref}}(s) = \frac{G(s)H_{n,0}(s)H'_{n,0}(s)}{1+G(s)H(s)H_{n,o}(s)H'_{n,0}(s)} \quad (22)$$

$$H_{n,\mathrm{osc}}(s) = \frac{H_{n,0}(s)H'_{n,0}(s)}{1+G(s)H(s)H_{n,0}(s)H'_{n,0}(s)} \quad (23)$$

$$H_{n,\mathrm{inj}}(s) = \frac{H_{n,i}(s)}{1+G(s)H(s)H_{n,0}(s)H'_{n,0}(s)}. \quad (24)$$

Note that in (22)–(24), $H'_{n,0}(s)$ is the inner self-injection-locked loop transfer function and is given as

$$H'_{n,0}(s) = \frac{1}{1+G'_{n,i}(s)(1-e^{-s\tau_i})\cos\phi}. \quad (25)$$

B. Applicable Parameters

This section characterizes how to adjust the inner self-injection locked parameters to compensate for the LO pulling effects. With the assistance of the proposed dual self-injection PLL model, the forecasted phase noise and EVMs results are compared with measurement results to account for the improved performance of the inner self-injection approach.

Fig. 10(a) and (b) plots the calculated magnitude response of the noise transfer functions $H_{n,\mathrm{inj}}(j\omega)$, $H_{n,\mathrm{osc}}(j\omega)$, and $H_{n,\mathrm{inj}}(j\omega)$ as the modulated outer self-injection power equals to -45 dBm. In these figures, the dotted lines in blue (in online version), broken lines in red (in online version), and solid lines in black express the responses with constant inner self-injection path delay of 20 ns and an injection angle of 180°. However, they are applied with various inner self-injection powers, which are equal to -20, -10, and -3, respectively. According to the above results, the magnitude of the dominant noise transfer function $H_{n,\mathrm{inj}}(j\omega)$ within the PLL bandwidth goes lower as the inner self-injection power increases, indicating that the impact of the PM injection noise is diminished with an increasing inner self-injection power.

Fig. 10(c)–(e) summarizes the measurement and calculation results of LO phase noise and EVM degradation under different inner self-injection powers. According to these figures, theoretical and experimental results coincide with each other up to a modulated outer self-injection power level of -45 dBm. Under identical LO pulling conditions, higher inner self-injection power implies a greater improvement of transmitted signal quality.

Notably, the applied GMSK signal is of narrow bandwidth so that the resulting angle $\alpha(t)$ in Adler's analysis is rather small. After inspection, the small-signal condition shown as

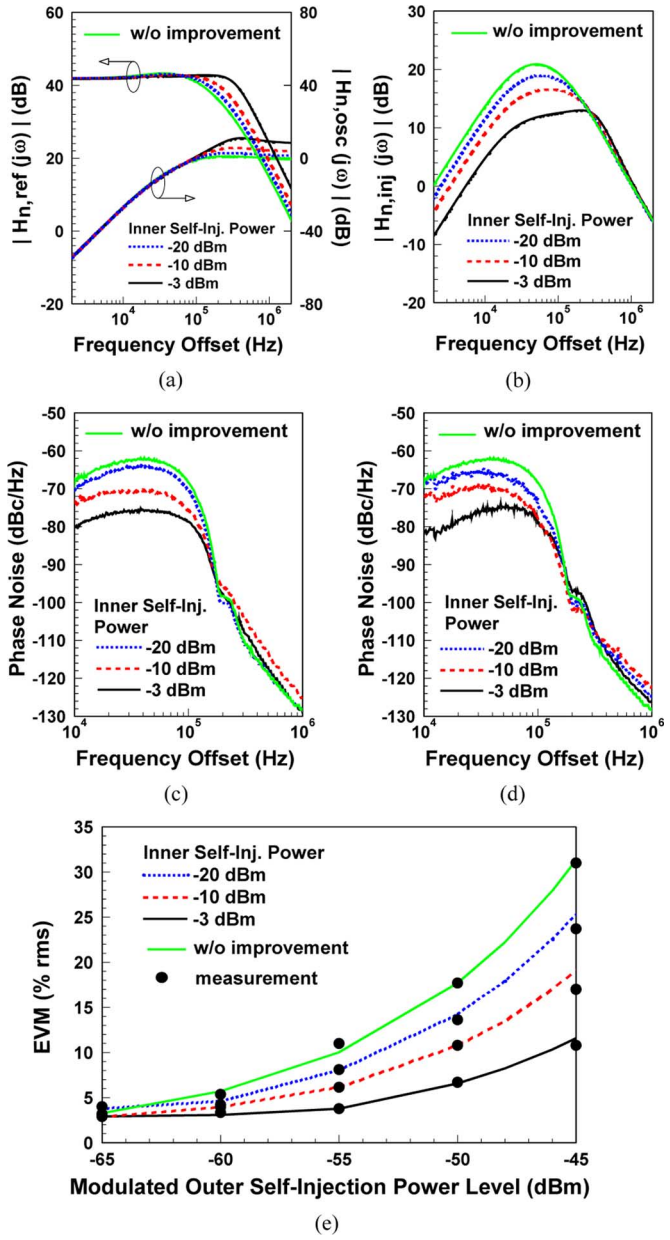

Fig. 10. Improvement of LO pulling effects and validation under various inner self-injection power levels. (a) Calculated magnitude of the reference and oscillator noise transfer functions. (b) Calculated magnitude of the PM injection noise transfer function. (c) Calculated LO phase noise. (d) Measured LO phase noise (e) Calculated and measured transmitter EVMs.

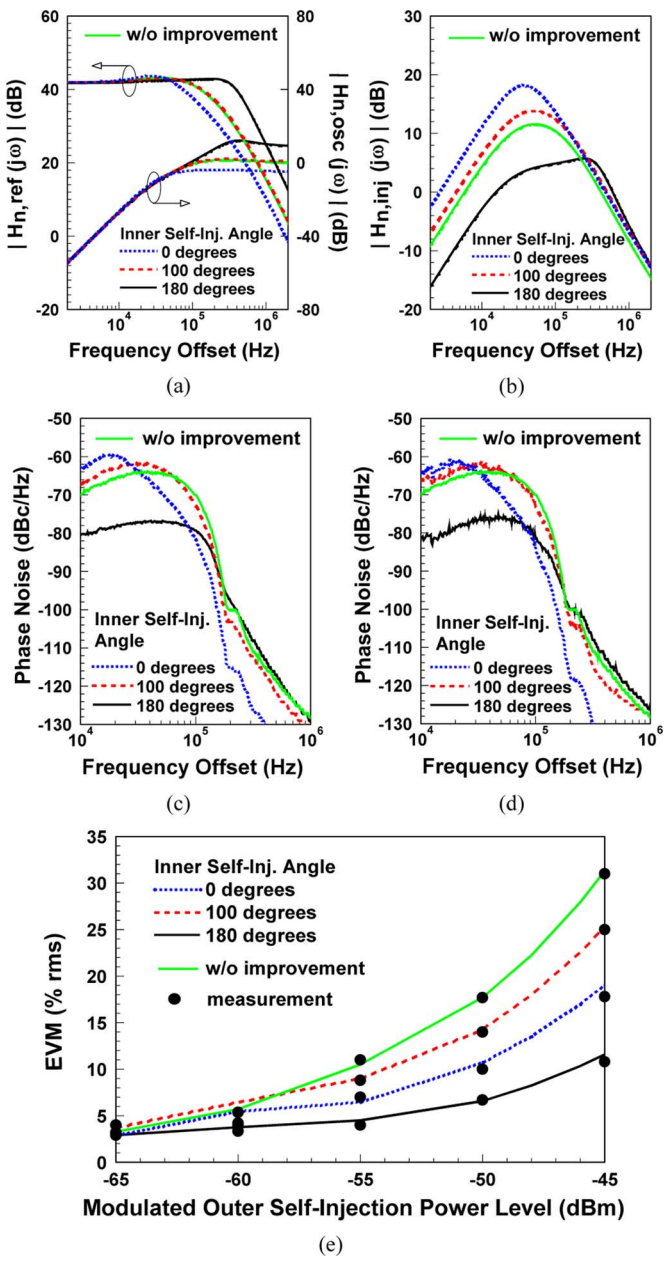

Fig. 11. Improvement of LO pulling effects and validation under various inner self-injection angles. (a) Calculated magnitude of the reference and oscillator noise transfer functions. (b) Calculated magnitude of the PM injection noise transfer function. (c) Calculated LO phase noise. (d) Measured LO phase noise (e) Calculated and measured transmitter EVMs.

$\sin\alpha(t) \ll 2QE_{\rm osc}/E_{\rm inj}$ still holds when the injection power increases up to -3 dBm. Therefore, the nonlinear effects are ignored for this case.

Fig. 11(a) and (b) plots the calculated magnitude response of the noise transfer functions $H_{n,\rm ref}(j\omega)$, $H_{n,\rm osc}(j\omega)$, and $H_{n,\rm inj}(j\omega)$ as the modulated outer self-injection power equals to -45 dBm. In these figures, the dotted lines in blue (in online version), broken lines in red (in online version), and solid lines in black express the responses with constant inner self-injection power of -3 dBm and path delay of 20 ns, but with different inner self-injection angles which are equal to 0°, 100°, and 180°, respectively. Fig. 11(c)–(e) illustrates the measurement and calculation results of LO phase noise and transmitted signal EVM degradation under different inner self-injection angles. An excellent correlation can be obtained from these figures, revealing that the different angles correspond to different phase noise improved areas. A situation in which the inner self-injection angle ϕ is approximated from 90° to 180° helps to diminish in-band phase noise, but slightly deteriorates the out-band phase noise, and, vice versa, with the angle approximately less than 90°. This tradeoff depends on the specification requirement of a realistic communication system. The optimum value for ϕ can be found by solving for the derivative of the PM injection noise transfer function shown in (24) equal to zero. This yields $\phi = 180°$ for the minimum transfer function magnitude.

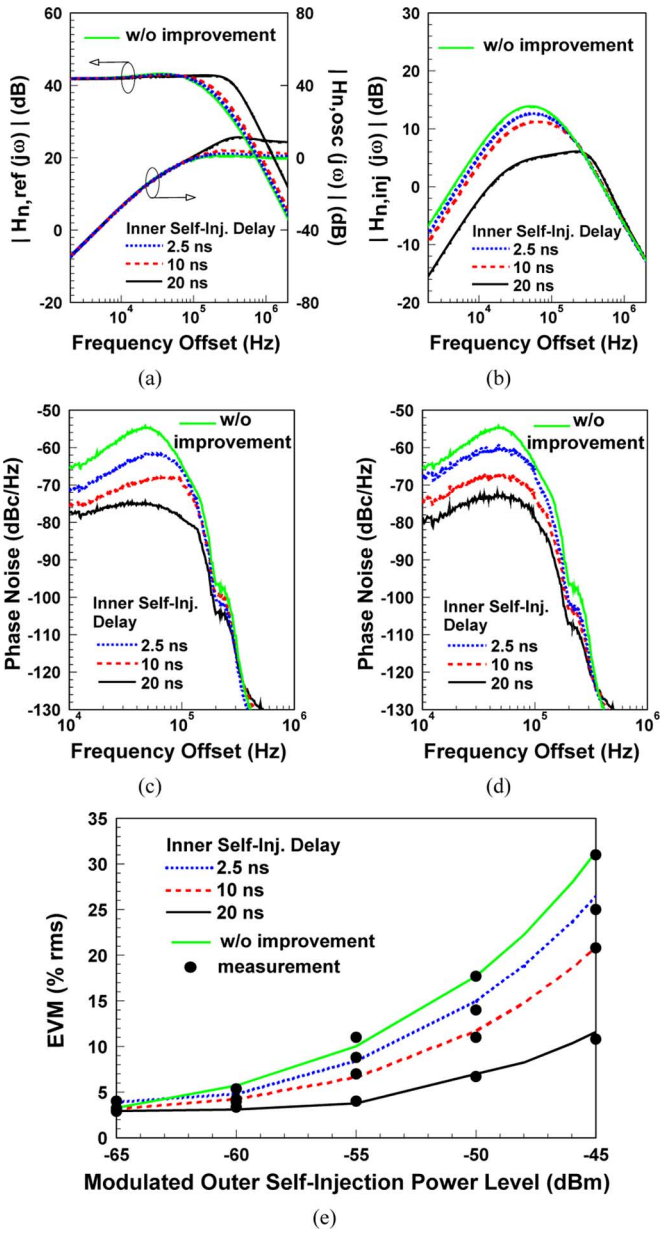

Fig. 12. Improvement of LO pulling effects and validation under various inner self-injection delays. (a) Calculated magnitude of the reference and oscillator noise transfer functions. (b) Calculated magnitude of the PM injection noise transfer function. (c) Calculated LO phase noise. (d) Measured LO phase noise (e) Calculated and measured transmitter EVMs.

Fig. 12(a) and (b) plots the calculated magnitude response of the noise transfer functions $H_{n,\mathrm{ref}}(j\omega)$, $H_{n,\mathrm{osc}}(j\omega)$, and $H_{n,\mathrm{inj}}(j\omega)$ as the injection pulling power equals to -45 dBm. In these figures, the dotted lines in blue (in online version), broken lines in red (in online version), and solid lines in black express the responses with constant inner self-injection power of -3 dBm and self-injection angle of 180°, but with different injection path delays, which are equivalent to 2.5, 10, and 20 ns, respectively. The measurement and calculation results of LO phase noise and transmitter EVM under different path delays are shown in Fig. 12(c)–(e). According to these figures, the LO phase noise and transmitter EVM are effectively improved with an increasing path delay. However, there are

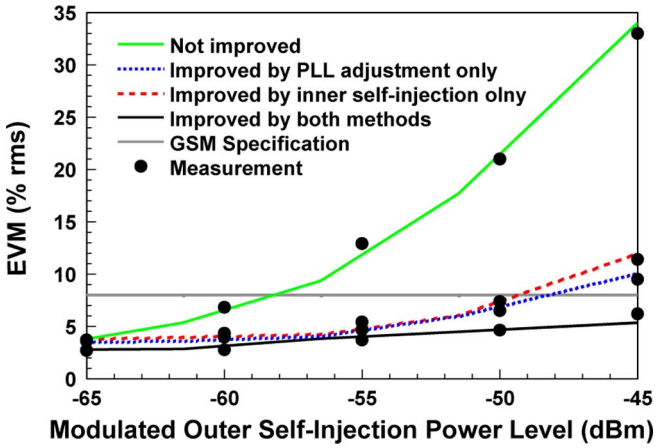

Fig. 13. Comparison of EVM performance by selecting different combinations of the PLL and inner self-injection parameters.

losses in actual delay lines, making it unlikely to achieve an arbitrary long delay without decaying injection power. It is noted that the inner self-injection approach on phase-noise reduction will not take into effects as the injection power decreases seriously.

Notably, the analyses in [25] and [27] consider the carrier phase delay via the self-injection path and find that the phase noise improvement is not monotonically increasing with the path delay. With different treatment, this work includes the carrier phase delay as part of the self-injection angle ϕ and evaluates the dependence of LO phase noise and transmitter EVM on the path delay at $\phi = 180°$, the optimum angle for minimizing the effect of PM injection noise. Under this optimum condition, this work theoretically and experimentally evidences that a longer path delay leads to a lower LO phase noise and transmitter EVM.

C. Optimal Design Strategy

The above theoretical analysis allows us to optimize the PLL parameters in order to alleviate the pulling effects. Moreover, an inner self-injection locked loop is introduced to enhance the transmitted signal quality. Based on the measurement results, we recommend that designers select a larger PLL bandwidth and phase margin together with applying the inner self-injection approach simultaneously for achieving the optimal pulling-effect resistance. Notably, the above hypothesis is made by assuming that altering these parameters does not affect the system stability.

Fig. 13 compares the performance of EVM with different proposed improved method combinations. In this figure, the dotted line in blue (in online version), broken line in red (in online version), and solid line in black represent the improved results by only adjusting the PLL parameters, by only applying the inner self-injection approach, and by performing above two approaches simultaneously, respectively. Additionally, the solid line in green (in online version) expresses the EVM results without applying any improvement procedure, and the solid line in gray depicts the EVM minimum specification requirement for GSM [29]. The measurement results correlate well with the theoretical analyzing ones. Furthermore, the EVMs are

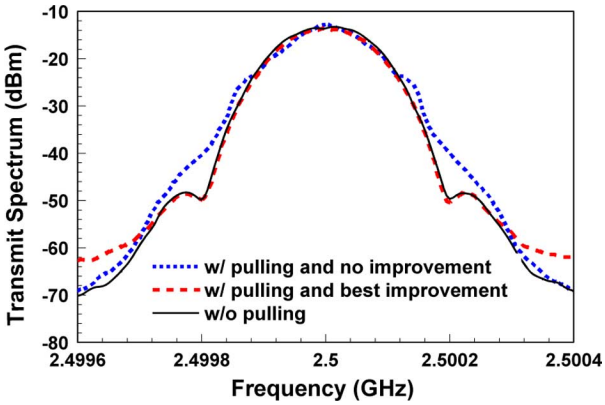

Fig. 14. Measured DCT output spectra for comparing the LO pulling effects between with and without improvement.

TABLE I
COMPARISON OF ACPR RESULTS

Measurement Bandwidth	30 kHz		
Frequency Offset	100 kHz	200 kHz	400 kHz
ACPR w.r.t. Pulled Spectrum	-9.6 dB	-21.8 dB	-54.1 dB
ACPR w.r.t. mproved Pulled Spectrum	-12.1 dB	-33.8 dB	-48.4 dB

significantly improved by a maximum value of around 30% as the modulated outer self-injection power equals to −45 dBm.

D. ACPR Performance

As mentioned in Section I, an LO is easily disturbed by the PA output modulation signal, subsequently inducing pulling effects to contaminate the spectral purity, and ultimately to degrade the transmitted signal quality. Fig. 14 displays how the pulling effects influence on transmitted output spectral regrowth at a modulated outer self-injection power of −45 dBm, while the dotted line in blue (in online version), broken line in red (in online version), and solid line in black represent the pulled, improved pulled, and unpulled spectrum, respectively. Comparison shows that severe spectral regrowth occurs in the pulled spectrum, but the phenomenon is significantly reduced by the proposed optimal design methodology, as can be seen in the improved pulled spectrum. Table I summarizes the comparison of the adjacent channel power ratio (ACPR) results. It shows that the proposed approach improves ACPR by 2.5 and 12 dB at the frequency offset of 100 and 200 kHz, respectively, but degrades the ACPR at a higher frequency offset. This is because the proposed approach mainly suppresses the in-band noise, but at a cost of slightly increasing the out-band noise.

V. CONCLUSION

By thoroughly elucidating how LO pulling affects a DCT that uses the GMSK modulation, this work presents a dual-loop phase dynamic model based on a directly modulated self-injection PLL to account for and predict the degradation of phase noise and signal quality due to the pulling effects. The calculation and measurement results correlate well with each other. A novel innovation is proposed to optimize the PLL parameters and introduce the inner self-injection locked loop to mitigate the pulling effects. With the assistance of both approaches, the EVM of the transmitter was effectively limited to 3%–5% up to a modulation injection power level of −45 dBm. Consequently, the directly modulated self-injection PLL analysis provides an effective means of characterizing the DCT pulling phenomenon. Moreover, the pulling effects can be successfully suppressed by executing the suggested optimal design strategy.

REFERENCES

[1] B. Razavi, "Challenges in portable RF transceiver design," *IEEE Circuits Devices Mag.*, vol. 12, no. 5, pp. 12–25, Sep. 1996.
[2] B. Razavi, "RF transmitter architectures and circuits," in *Proc. IEEE Custom Integr. Circuits Conf.*, San Diego, CA, 1999, pp. 197–204.
[3] R. E. Best, *Phase-Locked Loops: Theory, Design, and Applications*, 2nd ed. New York: McGraw-Hill, 1993.
[4] I. Krivokapic and M. Oskowsky, "GTEM cell method based comparative analysis of performance degradation in integer and fractional frequency synthesizer based direct conversion CDMA transmitters," in *Proc. Freq. Control Symp. and Expos.*, 2005, pp. 569–574.
[5] J. Dominguez, A. Suarez, and S. Sancho, "Semi-analytical formulation for the analysis and reduction of injection-pulling in front-end oscillators," in *IEEE MTT-S Int. Microw. Symp. Dig.*, Jun. 2009, pp. 1589–1592.
[6] R.-B. Staszewski, D. Leipold, and P.-T. Balsara, "Direct frequency modulation of an ADPLL for Bluetooth/GSM with injection pulling elimination," *IEEE Trans. Circuits Syst. II, Exp. Briefs*, vol. 52, no. 6, pp. 339–343, Jun. 2005.
[7] S. Mendel, C. Vogel, and N. D. Dalt, "A phase-domain all digital phase-locked architecture without reference clock retiming," *IEEE Trans. Circuits Syst. II, Exp. Briefs*, vol. 56, no. 11, pp. 860–864, Nov. 2009.
[8] I. Bashir, R.-B. Staszewski, O. Eliezer, K. Waheed, V. Zoicas, N. Tal, J. Mehta, M.-C. Lee, P.-T. Balsara, and B. Banerjee, "An EDGE transmitter with mitigation of oscillator pulling," in *IEEE Radio Freq. Integr. Circuit Symp. Dig.*, May 2010, pp. 13–16.
[9] R. Adler, "A study of locking phenomena in oscillators," *Proc. IRE*, vol. 34, no. 6, pp. 351–357, Jun. 1946.
[10] R. D. Huntoon and A. Weiss, "Synchronization of oscillators," *Proc. IRE*, vol. 35, no. 12, pp. 1415–1423, Dec. 1947.
[11] K. Kurokawa, "Noise in synchronized oscillators," *IEEE Trans. Microw. Theory Tech.*, vol. MTT-16, no. 4, pp. 234–240, Apr. 1968.
[12] K. Kurokawa, "Injection locking of microwave solid-state oscillators," *Proc. IEEE*, vol. 61, no. 10, pp. 1386–1410, Oct. 1973.
[13] X. Lai and J. Roychowdhury, "Automated oscillator macromodelling techniques for capturing amplitude variations and injection locking," in *Proc. IEEE/ACM Int. Comput.-Aided Design Conf.*, San Jose, CA, Nov. 2004, pp. 687–694.
[14] B. Razavi, "A study of injection locking and pulling in oscillators," *IEEE J. Solid-State Circuits*, vol. 39, no. 9, pp. 1415–1424, Sep. 2004.
[15] A. Mirzaei, M. E. Heidari, and A. A. Abidi, "Analysis of oscillators locked by large injection signals: Generalized adler's equation and geometrical interpretation," in *Proc. IEEE Custom Integr. Circuits Conf.*, San Jose, CA, Sep. 2006, pp. 737–740.
[16] M. E. Heidari and A. A. Abidi, "Behavioral models of frequency pulling in oscillators," in *Proc. IEEE Int. Behavioral Modeling Simulation Workshop*, San Jose, CA, Sep. 2007, pp. 100–104.
[17] P. Bhansali and J. Roychowdhury, "Gen-Adler: The generalized Adler's equation for injection locking analysis in oscillators," in *IEEE Asia–Pacific Microwave Conf.*, 2009, pp. 522–527.
[18] P. Maffezzoni and D. D'Amor, "Evaluating pulling effects in oscillators due to small-signal injection," *IEEE Trans. Comput.-Aided Des. Integr. Circuits Syst.*, vol. 28, no. 1, pp. 22–31, Jun. 2009.
[19] C.-J. Li, C.-H. Hsiao, F.-K. Wang, T.-S. Horng, and K.-C. Peng, "A rigorous analysis of a phased-locked oscillator under injection," in *IEEE Radio Freq. Integr. Circuits Symp. Dig.*, 2009, pp. 409–412.
[20] C.-J. Li, C.-H. Hsiao, F.-K. Wang, T.-S. Horng, and K.-C. Peng, "A rigorous analysis of a phased-locked oscillator under injection," *IEEE Trans. Microw. Theory Tech.*, vol. 58, no. 5, pp. 1391–1400, May 2010.
[21] C.-H. Hsiao, C.-J. Li, F.-K. Wang, T.-S. Horng, and K.-C. Peng, "Study of direct-conversion transmitter pulling effects in constant envelope modulation systems," in *IEEE MTT-S Int. Microw. Symp. Dig.*, May 2010, pp. 1174–1177.
[22] H.-C. Chang, A. Borgioli, P. Yeh, and R.-A. York, "Analysis of oscillators with external feedback loop for improved locking range and noise reduction," *IEEE Trans. Microw. Theory Tech.*, vol. 47, no. 8, pp. 1535–1543, Aug. 1999.

[23] L. Pan, Y. Bar-Ness, and J. Zhu, "Effects of phase noise at both transmitter and receiver on the performance of OFDM systems," in *Proc. 40th Annu. Inform. Sci. Syst. Conf.*, Mar. 2006, pp. 312–316.
[24] D. Banerjee, *PLL Performance, Simulation, and Design*, 4th ed. Indianapolis, IN: Dog Ear Publishing, 2006.
[25] H.-C. Chang, "Stability analysis of self-injection-locked oscillators," *IEEE Trans. Microw. Theory Tech.*, vol. 51, no. 9, pp. 1989–1993, Sep. 2003.
[26] H.-C. Chang, "Phase noise in self-injection-locked oscillators-theory and experiment," *IEEE Trans. Microw. Theory Tech.*, vol. 51, no. 9, pp. 199–1994, Sep. 2003.
[27] A. Suarez and F. Ramirez, "Analysis of stabilization circuits for phase-noise reduction in microwave oscillators," *IEEE Trans. Microw. Theory Tech.*, vol. 53, no. 9, pp. 2743–2751, Sep. 2005.
[28] T.-P. Wang, Z.-M. Tsai, K.-J. Sun, and H. Wang, "Phase noise reduction of X-band push–push oscillator with second-harmonic self-injection techniques," *IEEE Trans. Microw. Theory Tech.*, vol. 55, no. 1, pp. 66–77, Jan. 2007.
[29] "Understanding GSM/EDGE transmitter and receiver measurements for base transceiver stations and their components," Agilent Technol., Santa Clara, CA, Appl. Note 1312, 2002.

Chieh-Hsun Hsiao (S'10) was born in Kaohsiung, Taiwan, on June 5, 1984. He received the B.S.E.E. and M.S.E.E. degrees from National Sun Yat-Sen University, Kaohsiung, Taiwan, in 2006 and 2008, respectively, and is currently working toward the Ph.D. degree in electrical engineering at National Sun Yat-Sen University. His doctoral research concerns phase- and injection-locked oscillators.

Chien-Jung Li (S'07–M'10) was born in Tainan, Taiwan, on October 26, 1979. He received the B.S.E.E. and Ph.D. degrees from National Sun Yat-Sen University, Kaohsiung, Taiwan, in 2002 and 2009, respectively.

He is currently a Postdoctoral Fellow with the Department of Electrical Engineering, National Sun Yat-Sen University. His research interests include PA linearization techniques, frequency synthesizer designs, and LO pulling issues in direct-conversion transceivers.

Fu-Kang Wang (S'10) was born in Kaohsiung, Taiwan, on May 15, 1985. He received the B.S.E.E. and M.S.E.E. degrees from National Sun Yat-Sen University, Kaohsiung, Taiwan, in 2007 and 2009, respectively, and is currently working toward the Ph.D. degree in electrical engineering at National Sun Yat-Sen University. His doctoral research concerns RF sensing techniques.

Tzyy-Sheng Horng (S'88–M'92–SM'05) was born in Taichung, Taiwan, on December 7, 1963. He received the B.S.E.E. degree from National Taiwan University, Taipei, Taiwan, in 1985, and the M.S.E.E. and Ph.D. degrees from the University of California at Los Angeles (UCLA), in 1990 and 1992, respectively.

Since August 1992, he has been with the Department of Electrical Engineering, National Sun Yat-Sen University, Kaohsiung, Taiwan, where he was the Director of the Telecommunication Research and Development Center (2003–2008) and Director of the Institute of Communications Engineering (2004–2007), and where he is currently a Professor. He has authored or coauthored over 100 technical publications published in refereed journals and conferences proceedings. He holds over ten patents. His research interests include RF and microwave integrated circuits and components, RF signal integrity for wireless system-in-package, and digitally assisted RF technologies.

Dr. Horng has served on several Technical Program Committees of international conferences including the International Association of Science and Technology for Development (IASTED) International Conference on Wireless and Optical Communications, the IEEE Region 10 International Technical Conference, the IEEE International Workshop on Electrical Design of Advanced Packaging and Systems, the Asia–Pacific Microwave Conference, the IEEE Radio and Wireless Symposium, and the Electronic Components and Technology Conference. He was the recipient of the 1996 Young Scientist Award presented by the International Union of Radio Science, the 1998 Industry–Education Cooperation Award presented by the Ministry of Education, Taiwan, and the 2010 Distinguished Electrical Engineer Award presented by the Chinese Institute of Electrical Engineering, Taiwan.

Kang-Chun Peng (S'00–M'05) was born February 18, 1976, in Taipei, Taiwan. He received the B.S.E.E., M.S.E.E., and Ph.D. degrees from National Sun Yat-Sen University, Kaohsiung, Taiwan, in 1998, 2000, and 2005, respectively.

He is currently an Assistant Professor with the Department of Computer and Communication Engineering, National Kaohsiung First University of Science and Technology, Kaohsiung, Taiwan. His current research interests are in the area of delta–sigma modulation techniques, low-noise PLLs, low-power VCOs, and modulated frequency synthesizers.